

# UHECRs from magnetic reconnection in relativistic jets

Dimitrios Giannios<sup>\*</sup>

*Department of Astrophysical Sciences, Peyton Hall, Princeton University, Princeton, NJ 08544, USA*

Received / Accepted

## ABSTRACT

Ultra-high-energy cosmic rays (UHECRs) may be produced in active galactic nuclei (AGN) or gamma-ray burst (GRB) jets. I argue that magnetic reconnection in jets can accelerate UHECRs rather independently of physical processes in the magnetic dissipation region. First order Fermi acceleration can efficiently take place in the region where the unreconnected (upstream) magnetized fluid converges into the reconnection layer. I find that protons can reach energies up to  $E \sim 10^{20}$  eV in GRB and powerful AGN jets while iron nuclei can reach similar energies in AGN jets of more moderate luminosity.

**Key words:** Cosmic rays: ultra-high energies – gamma rays: bursts – galaxies: active – magnetic reconnection

## 1 INTRODUCTION

The origin of UHECRs (particles with energy  $E \gtrsim 10^{19}$  eV) remains a mystery. The fact that magnetic fields cannot confine them in the Galaxy and the observed spectral cutoff at  $\sim 6 \times 10^{19}$  eV point to extragalactic sources at these energies (Abbasi et al. 2008; Abraham et al. 2008). For any astrophysical source to accelerate particles to the highest observed energies of  $E_M \gtrsim 10^{20}$  eV, tight constraints need to be satisfied. Possibly, the tightest come from the need for particles with energy  $E_M$  to be confined within the size of the source (Hillas 1984) and the acceleration to take place within the available (dynamical) time of the system. Both constraints may be met in very powerful sources. Viable astrophysical sources for UHECRs are relativistic jets from active galactic nuclei (see, e.g. Halzen & Hooper 2002) and gamma-ray bursts (Milgrom & Usov 1995; Waxman 1995; Vietri 1995; see, however, Ghisellini et al. 2008; Inoue 2008 for alternatives).

The acceleration mechanism for UHECRs is usually postulated to be the first order Fermi mechanism in (mildly) relativistic shocks in the jets (because of internal or external interactions; Gallant & Achterberg 1999; Achterberg et al. 2001). For the UHECRs to be confined by shocks both the upstream and downstream need to be strongly magnetized (i.e. with magnetic energy density not much less than the total energy density; e.g. Waxman 1995). The magnetic fields cannot be of small scale (generated by plasma instabilities) since in this case the small angle scattering of the energetic particles makes the acceleration process too slow to be of relevance (Kirk & Reville 2010). Strong, large scale fields are also unlikely to work since they do not allow for the particles to repeatedly cross the shock front (where the acceleration takes place) for most field inclinations (e.g. Sironi & Spitkovsky 2009).

Here I discuss an alternative mechanism for UHECR acceleration in a relativistic flow. This mechanism applies to magnetic reconnection regions in Poynting-flux dominated flows (e.g. flows with Poynting-to-kinetic flux ratio  $\sigma \gtrsim 1$ ). The particle acceleration takes place through the first order Fermi mechanism because of particles reflected in the magnetized plasma that is converging in the reconnection region (see Speiser 1965 and de Gouveia dal Pino & Lazarian 2005 for a similar mechanism applied to Earth's magnetotail and the ejections from the microquasar GRS 1915+105 respectively). The strong, large scale field in the upstream of the reconnection region that approaches the reconnection layer at subrelativistic speed results in a very efficient acceleration configuration.

In the next section, I describe the mechanism for particle acceleration to ultra-high energies. This mechanism is applied to relativistic jets in Sect. 3. Discussion is given in Sect. 4.

## 2 PARTICLE ACCELERATION IN MAGNETIC RECONNECTION REGIONS

In this work, I do not assume any specific mechanism for magnetic reconnection. I consider the rather generic geometry where magnetized fluid with reversing polarity over a lengthscale  $l_{\text{rec}}$  is advected into the dissipation layer with speed  $\beta_{\text{rec}} = v_{\text{rec}}/c$ . The plasma is heated/compressed and accelerated by the released magnetic energy and leaves the region through a narrow layer of thickness  $\delta \ll l_{\text{rec}}$  at the Alfvén speed of the upstream plasma  $\beta_{\text{out}} \sim \beta_A$  (e.g. Lyubarsky 2005; see fig. 1). For high  $\sigma$  flows considered here  $\beta_{\text{out}} \sim 1$ .

Particle acceleration at the reconnection layer can be complicated by the exact, small-scale reconnection geometry. At the location where magnetic energy is dissipated one may deal with current sheets (Parker 1957; Sweet 1958), slow MHD shocks (Petschek

<sup>\*</sup> E-mail: giannios@astro.princeton.edu

1964; Zenitani, Hesse & Klimas 2009), MHD turbulence (Lazarian & Visniak 1999; Matthaeus & Lamkin 1986; Loureiro et al. 2009) and/or secondary tearing instabilities (Drake et al. 2006; Loureiro, Schekochihin & Cowley 2007; Samtaney et al. 2009). Regardless of the details of the reconnection mechanism, however, any successful reconnection model must explain the observed fast rate with which magnetic field lines are advected into the reconnection region (e.g. Lin et al. 2003). The so-called reconnection speed has to be a substantial fraction (a tenth or so) of the Alfvén speed  $\beta_A$  of the upstream plasma. For  $\beta_A \sim 1$  the reconnection speed is subrelativistic:  $\beta_{\text{rec}} \equiv \epsilon \sim 0.1$ .

I assume that a preacceleration mechanism is able to accelerate ions to large enough energy so that their gyroradius  $R_g$  becomes larger than the thickness of the layer  $\delta$ . Such preacceleration may take place in contracting magnetic islands (Drake et al. 2006), current sheets (e.g. Kirk 2004) or slow MHD shocks. After the initial acceleration (discussed in Sect. 3.3), the particle trajectories and energy will be subject to at most mild change while they cross the dissipation layer. Still, as long as  $R_g \lesssim l_{\text{rec}}$ , the particles are confined in the wider reconnection region and can be accelerated further.

## 2.1 The acceleration cycle

The acceleration of the particles in the reconnection region may be viewed from two equivalent perspectives. In the rest frame of the current layer, the upstream region contains an advective electric field directed along the  $x$  axis of strength  $\mathcal{E}_x = \beta_{\text{rec}} B$  (the so-called reconnection electric field). A particle bounces back and forth around the reconnection layer in a betatron-like orbit (also called Speiser orbit) schematically shown in Fig. 1. It is continuously accelerated by the electric field with its energy increasing linearly with distance  $x$  traveled along the layer  $E' \sim e\beta_{\text{rec}} Bx$  (Speiser 1965). The acceleration may also be viewed as result of repeated magnetic reflections in the upstream flow. The fact that the upstream is converging towards the dissipation region, allows for a first order Fermi acceleration to operate (de Gouveia dal Pino & Lazarian 2005). As a result, particles gain a fixed fractional energy per cycle that can be estimated by the following considerations (that involve two Lorentz boosts).

Consider that a particle of Lorentz factor  $\gamma_1 \gg 1$  (measured in, e.g., the lower side of the upstream region; see Fig. 1) enters at an angle  $\theta$  (with respect to the normal to the reconnection layer, i.e., the  $y$  axis) into the opposite side of the upstream. The relative speed of the two regions is

$$\beta_r = \frac{2\beta_{\text{rec}}}{1 + \beta_{\text{rec}}^2}. \quad (1)$$

The Lorentz factor  $\gamma_2$  of the same particle measured in the rest frame of the upper side is given by the transformation  $\gamma_2 = \gamma_1 \gamma_r (1 + \beta_r \cos \theta)$ . The particle performs a fraction of a gyration and leaves the upper side at an angle  $-\theta$ .<sup>1</sup> The particle completes the cycle by returning to the lower region with Lorentz factor (in the rest frame of that region)  $\gamma_3 = \gamma_2 \gamma_r (1 + \beta_r \cos \theta)$ . The amplification in energy during the  $1 \rightarrow 2 \rightarrow 1$  cycle is

<sup>1</sup> In general the particle will return at an angle  $|\theta'|$  different than  $\theta$ . The change in the angle is small during a single cycle for subrelativistic  $\beta_{\text{rec}}$  discussed here and can be ignored. Furthermore, a small deflection of the particle may take place while it crosses the reconnection layer that introduces some degree stochasticity to the orbit but does not affect the main arguments presented here.

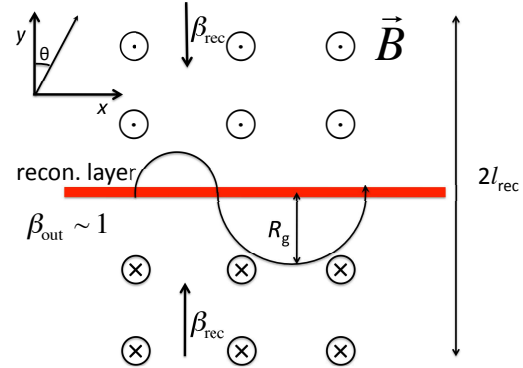


**Figure 1.** Sketch of the reconnection geometry. High- $\sigma$  plasma approaches the reconnection layer at subrelativistic speed  $\beta_{\text{rec}}$  from both sides (upstream flow). Plasma leaves the region through a thin layer with  $\beta_{\text{out}} \sim 1$  perpendicular to the plane of the sketch (downstream flow). Energetic ions are Fermi accelerated by being repeatedly reflected by the upper and lower sides of the upstream.

$$A(\theta) \equiv \frac{\gamma_3}{\gamma_1} = \gamma_r^2 (1 + \beta_r \cos \theta)^2. \quad (2)$$

In the limit of  $\theta = 0$  (particle crossing perpendicular to the reconnection layer), the amplification  $A$  is given as function of  $\beta_{\text{rec}}$ :

$$A(0) = \frac{1 + \beta_r}{1 - \beta_r} = \frac{(1 + \beta_{\text{rec}})^2}{(1 - \beta_{\text{rec}})^2}, \quad (3)$$

where eq. (1) is used in the last step. If any scattering process (e.g. when crossing the reconnection layer) keeps the particle distribution quasi-isotropic, particles will cross the dissipation region with a angular probability distribution  $P(\theta)d\theta = 2 \sin \theta \cos \theta d\theta$  with  $0 \leq \theta \leq \pi/2$ . In this case, the average amplification per circle is

$$\langle A \rangle = \int_0^{\pi/2} A(\theta) P(\theta) d\theta = \gamma_r^2 \left[ 1 + \frac{4}{3} \beta_r + \frac{1}{2} \beta_r^2 \right]. \quad (4)$$

Note that, in the limit  $\beta_{\text{rec}} \ll 1$ ,  $\langle A \rangle = 1 + 8\beta_{\text{rec}}/3$  as found in de Gouveia dal Pino & Lazarian (2005).

In Fig. 2, I plot the  $A(0)$  and  $\langle A \rangle$  as a function of  $\beta_{\text{rec}}$ . Note that  $A(0)$  and  $\langle A \rangle$  have rather similar values making the results that follow rather insensitive to the exact angular distribution of the particles. One can see that for reasonable values of  $\beta_{\text{rec}} \sim 0.2$ , amplification of factor of  $\sim 2$  is expected.

## 2.2 Acceleration time scale

One acceleration cycle for a particle of energy  $\gamma$  approximately equals the gyration time  $t_g = 2\pi m c^2 / e B c$  at this energy<sup>2</sup>, where  $m$  is the mass of the particle and  $B$  the magnetic field strength of the upstream region. At the previous cycle the particle has  $A^{-1}$  less energy (and the cycle lasts proportionally shorter). The total time (acceleration time) for a particle of Lorentz factor  $\gamma$  is the sum of the time spent in all the cycles until it reaches  $\gamma$ :

<sup>2</sup> The energy changes moderately during the cycle; we consider the final energy of the particle during the cycle slightly overestimating the gyration timescale and therefore the acceleration time.

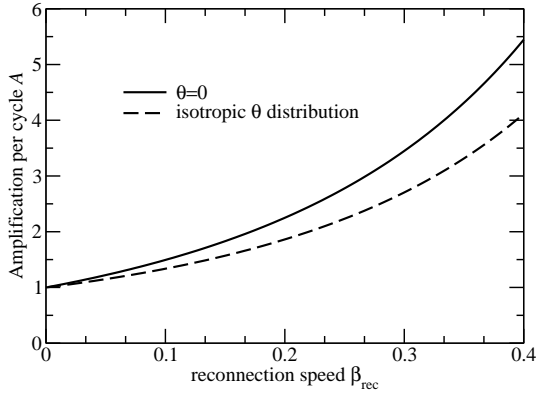


**Figure 2.** Energy amplification  $A$  of particles for every Fermi acceleration cycle as function of the reconnection speed  $\beta_{\text{rec}}$ . The solid curve corresponds to particles crossing the reconnection layer at an angle  $\theta = 0$  and the dashed curve to an isotropic particle distribution.

$$t_{\text{acc}} = \frac{2\pi\gamma mc^2}{eBc} (1 + A^{-1} + A^{-2} + \dots) = \frac{2\pi\gamma mc^2}{(1 - 1/A)eBc}. \quad (5)$$

For reasonable reconnection rates, the amplification is  $A \sim 2$  which corresponds to acceleration taking place at a timescale of the order of the gyration period for the maximum energy of the particles.

For a particle moving at a small angle with respect to the  $x$  direction ( $\theta \sim \pi/2$  case), the acceleration time scale can be estimated by setting the energy of the particle  $\gamma mc^2$  equal to  $e\beta_{\text{rec}} Bx$ , where  $x$  is the distance travelled along the layer. The acceleration time is, therefore,  $t_{\text{acc}} \approx x/c = \gamma mc^2 / (e\beta_{\text{rec}} Bc)$ . For  $\beta_{\text{rec}} \sim 0.1 - 0.2$ , the previous expression results in  $t_{\text{acc}} \sim t_g$ . This estimate is similar to that of eq. (5) showing that the  $\theta$  distribution of the particles has little effect on the timescale for particle acceleration.

### 3 CONSTRAINTS ON THE MAXIMUM PARTICLE ENERGY

A number of physical processes can limit the maximum energy that a particle acquires. The acceleration ceases once the dynamical timescale of the system becomes comparable to the acceleration time  $t_{\text{acc}}$  or when the particle can no longer be confined within the reconnection region or when cooling of the particle is fast enough to inhibit further acceleration. Each of these processes is discussed in turn.

In the following estimates, the magnetic field strength of the jet plays a critical role. It is determined by the (Poynting) luminosity  $L$ , bulk Lorentz factor  $\Gamma$  of the jet and the distance  $R$  from the central engine:

$$B = \frac{L^{1/2}}{c^{1/2} R \Gamma}, \quad (6)$$

where the magnetic field  $B$  strength is measured in the rest frame of the jet. For observed energy  $E$  of a UHECR, the energy of the particle in the rest frame of the jet is  $E' = E/\Gamma = \gamma mc^2$ . Throughout this work, we consider proton acceleration, i.e.  $m = m_p$  (the somewhat relaxed constraints for acceleration of heavier nuclei are straightforward to derive).

**Confinement Constraints:** for the particle to be confined within the reconnection region, the gyroradius  $R_g$  cannot exceed

the region's thickness  $l_{\text{rec}}$ .<sup>3</sup> Setting  $R_g = l_{\text{rec}}$  and using eq. (6) I find that

$$E_M^{\text{conf}} = \frac{e l_{\text{rec}}}{R} \sqrt{\frac{L}{c}}. \quad (7)$$

During their acceleration drift along the  $x$  direction, the particles may eventually leave the reconnection region. For a given length of the reconnection layer  $l_x$  the maximum energy that can be achieved is  $E_M = \Gamma e \beta_{\text{rec}} B l_x = e \beta_{\text{rec}} l_x (L/c)^{1/2} / R$ . For  $l_x \sim l_{\text{rec}}$ , the last expression gives a maximal energy that is a factor  $\beta_{\text{rec}}$  smaller than  $E_M^{\text{conf}}$ . On the other hand, in the model that is discussed in the next section,  $l_x$  is sufficiently larger than  $l_{\text{rec}}$  and the escape along the layer is no more constraining for the maximum energy than the estimate of eq. (7).

Scattering processes can lead to particle motion perpendicular to the plane of Fig. 1 (along the reconnecting magnetic field; i.e., along the  $z$  axis). Escape of particles in the  $z$  direction will depend on the size of the layer  $l_z$  and the nature of the scattering process. Particle escape in this direction is likely a stochastic process and may (in connection to the amplification per cycle  $A$ ) determine the distribution function of the accelerated particles but does not limit the maximum achieved energies.

**Cooling constraint:** the accelerated protons cool through synchrotron emission and photo-pion production. Both of these processes can limit the energy of the UHECRs. In practise, however, it can be shown that cooling is dominated by the synchrotron emission (Waxman 1995). The proton-synchrotron cooling timescale  $t_{\text{syn}} \approx \frac{3m_p^2 c^7 \Gamma}{e^4 B^2 E}$  can be set equal to the gyration time  $2\pi E / e c \Gamma B$  to derive

$$E_M^{\text{syn}} = \sqrt{\frac{3}{2\pi e^3 B}} (m_p c^2)^2 \Gamma = \sqrt{\frac{3R}{2\pi e^3}} (m_p c^2)^2 \Gamma^{3/2} \left(\frac{L}{c}\right)^{-1/4}, \quad (8)$$

where eq. (6) is used in the last step of the derivation.

**Timescale constraint:** The time available for the acceleration process to take place is limited by the dynamical (expansion) timescale of the jet. Equating the time  $R/\Gamma c$  that takes for the jet to double its radius (in its rest frame) to the acceleration time (taking it equal to the gyration time; see Sect. 2.2), one finds

$$E_M^{\text{time}} = \frac{e}{2\pi\Gamma} \sqrt{\frac{L}{c}}. \quad (9)$$

In the next section, these constraints are applied to specific sources.

#### 3.1 GRB jets

GRB jets have been proposed as sources of UHECRs by Milgrom & Usov (1995), Waxman (1995), and Vietri (1995) (see also Rieger & Duffy 2005; Murase et al. 2006; 2008). Using the observed long-duration GRB rate (e.g., Guetta, Piran & Waxman 2005) the energy release in  $\gamma$ -rays from bursts at the local Universe can be estimated to be  $\sim 10^{44} \text{ erg/Mpc}^3 \text{ yr}$ . This is comparable to the rate of energy release required to power the observed UHECRs with  $E \gtrsim 10^{19} \text{ eV}$  (Waxman 1995). GRBs are, thus, an energetically viable source *provided* that they can accelerate UHECRs with similar efficiency to which they produce  $\gamma$ -rays.

The (isotropic equivalent)  $\gamma$ -ray energy of long-duration

<sup>3</sup> This constraint may be somewhat relaxed if the particles move predominantly along the reconnection layer ( $\theta \sim \pi/2$ ) while been accelerated by the advective electric field.

GRBs are  $E_\gamma \sim 10^{53}$  erg while their duration is  $\sim 10$  s. This corresponds to typical  $\gamma$ -ray luminosity of  $L_\gamma \sim 10^{52}$  erg/s. During the active GRB phases, the luminosity of the jet is larger because of the likely moderate efficiency  $\lesssim 50\%$  in producing  $\gamma$ -rays, and the quiescent intervals in between ejection events. Here, I conservatively assume typical flow luminosity of  $L \sim 10^{52}$  erg/s. Furthermore, compactness arguments (e.g. Lithwick & Sari 2001) bring the bulk Lorentz factor of the flow into the hundreds:  $\Gamma \sim 100 - 1000$ .

Normalising  $L = 10^{52} L_{52}$  erg/s,  $\Gamma = 10^{2.5} \Gamma_{2.5}$  and the dissipation radius (to be estimated below) to  $R = 10^{13} R_{13}$  cm, the cooling and timescale constraints (8) and (9) read  $E_M^{\text{conf}} = 7 \times 10^{19} \Gamma_{2.5}^{3/2} R_{13}^{1/2} L_{52}^{-1/4}$  eV and  $E_M^{\text{syn}} = 9 \times 10^{19} L_{52}^{1/2} \Gamma_{2.5}^{-1}$  eV respectively. The last expressions show that proton energies of  $E \sim 10^{20}$  eV are within reach if the magnetic reconnection takes place at large enough distance.

The efficient dissipation of magnetic energy through reconnection presumes that the jet contains regions with reversing magnetic fields. These field reversals may be imprinted in the flow from the jet launching region (i.e. one deals with a non-axisymmetric rotator at the central engine) or are developed further out in the flow because of MHD instabilities. In the former case (i.e., that of an oblique rotator), the length scale of field reversals can be straightforwardly estimated to be (in the lab frame) of order of the light-cylinder of the central engine  $l_{\text{rec}}^{\text{lab}} \simeq c T_{\text{CE}}$ , where  $T_{\text{CE}}$  is the rotation period of the central engine. In the rest frame of the flow, the field reversal takes place on a scale  $l_{\text{rec}} = \Gamma l_{\text{rec}}^{\text{lab}} = \Gamma c T_{\text{CE}}$  (see, e.g., Drenkhahn 2002). In this picture, reconnection takes place over a range of distances but is completed at a distance  $R_{\text{rec}}$  for which the time scale of reconnection  $l_{\text{rec}}/\epsilon c$  equals the expansion timescale  $R/\Gamma c$ . Assuming a millisecond period rotator as the central engine of the GRB, the reconnection radius is (see Drenkhahn & Spruit 2002 for a more detailed derivation)

$$R_{\text{rec}} = \frac{\Gamma^2 c T_{\text{CE}}}{\epsilon} = 3 \times 10^{13} \frac{\Gamma_{2.5}^2 T_{-3}}{\epsilon_{-1}} \text{ cm.} \quad (10)$$

Using the last expression for the dissipation radius *predicted* by the reconnection model, one can write down the various constraints (7), (8), and (9) as

$$\begin{aligned} E_M^{\text{conf}} &= 6 \times 10^{19} \frac{\epsilon_{-1} L_{52}^{1/2}}{\Gamma_{2.5}} \text{ eV,} \\ E_M^{\text{syn}} &= 1.2 \times 10^{20} \frac{\Gamma_{2.5}^{5/2} T_{-3}^{1/2}}{L_{52}^{1/4} \epsilon_{-1}^{1/2}} \text{ eV,} \\ E_M^{\text{time}} &= 9 \times 10^{19} \frac{L_{52}^{1/2}}{\Gamma_{2.5}} \text{ eV.} \end{aligned} \quad (11)$$

Interestingly, for  $\epsilon \simeq 0.15$  the first and third constraints give the same result. Proton energies up to  $E \sim 10^{20}$  eV are plausible.

In this model, UHECRs are accelerated at a distance  $R_{\text{rec}}$  (see eq. (10)) which is much shorter than the distance where the jet decelerates interacting with the external medium. Adiabatic losses could, therefore, reduce the energy with which the particles escape. However, because of the efficient dissipation of Poynting flux at  $R_{\text{rec}}$ , the magnetic field strength drops with distance steeper than  $R^{-1}$  for  $R \gtrsim R_{\text{rec}}$ . It is, therefore, reasonable to assume that at least the most energetic particles become effectively decoupled from the jet and avoid adiabatic cooling. Note that in models for UHECR acceleration where the flow maintains a fixed fraction of Poynting flux, the magnetic field strength scales as  $B \propto 1/R$  (see eq. (6)). In those models, after the particle acceleration is completed  $R_g/ct_{\text{dyn}} \propto (RB)^{-1} = \text{const.}$ ; even very energetic particles remain coupled to the flow potentially suffering severe adiabatic losses.

### 3.2 Jets in active galactic nuclei

Powerful AGN jets can also potentially accelerate protons to UHECRs. Since we are not aware of any such jet with, say,  $L \sim 10^{48}$  erg/s within the Greisen, Zatsepin Kuzmin (GZK) radius (Greisen 1966; Zatsepin & Kuz'min 1966), one has to assume that such sources are transient (see Waxman & Loeb 2009 for discussion on observational constraints on the existence of sufficient number of AGN jets to power the observed UHECRs). A powerful AGN jet of  $L \sim 10^{48}$  erg/s and bulk  $\Gamma \sim 3$  that contains field reversals on scales  $l_{\text{rec}} \sim c T_{\text{CE}}$  with  $T_{\text{CE}} \sim 10^5$  s (i.e. some 8 orders of magnitude longer than that of the GRB central engine due to the larger mass of the compact object) can also satisfy the basic constraints for proton acceleration to the highest observed energies. For parameters relevant for AGN jets, eq. (11) gives:

$$\begin{aligned} E_M^{\text{conf}} &= 6 \times 10^{19} \frac{\epsilon_{-1} L_{48}^{1/2}}{\Gamma_{0.5}} \text{ eV,} \\ E_M^{\text{syn}} &= 1.2 \times 10^{20} \frac{\Gamma_{0.5}^{5/2} T_5^{1/2}}{L_{48}^{1/4} \epsilon_{-1}^{1/2}} \text{ eV,} \\ E_M^{\text{time}} &= 9 \times 10^{19} \frac{L_{48}^{1/2}}{\Gamma_{0.5}} \text{ eV.} \end{aligned} \quad (12)$$

It remains, however, to be shown that such powerful jets are occasionally activated in nearby AGNs (see Farrar & Gruzinov 2009 for a proposed mechanism for such AGN flares).

Unlike the GRB flow that is expected to consist of protons (and maybe neutrons) because of the extreme temperatures and densities of the launching region, AGN jets may contain heavier nuclei such as iron. For iron composition of the UHECRs, the constraints for acceleration on the luminosity of the source are significantly relaxed (see, e.g., Pe'er, Murase, Mészáros 2009; Honda 2009; Dermer & Rozaque 2010). Magnetic reconnection in less powerful AGN jets of  $L \sim 10^{44} - 10^{46}$  erg/s can accelerate iron up to energies of  $10^{20}$  eV.

### 3.3 Injection energy

The particles that enter the acceleration cycle discussed here, have passed through a preacceleration phase that makes their gyration radius  $R_g$  comparable to the thickness of the layer  $\delta$ . The required energy of the preacceleration phase depends on the details of the reconnection geometry but may be roughly estimated by the following considerations. Plasma of density  $\rho_{\text{in}}$  enters the reconnection region with speed  $\beta_{\text{rec}}$  and leaves it with density  $\rho_{\text{out}}$  at the Alfvén speed  $\beta_A = \sqrt{\sigma/(1+\sigma)}$  through the layer:  $\beta_{\text{rec}} \rho_{\text{in}} l_{\text{rec}} = \gamma_A \beta_A \rho_{\text{out}} \delta$ , where the length of the layer is assumed  $l_z \sim l_{\text{rec}}$ . The compression  $\rho_{\text{out}}/\rho_{\text{in}}$  in the layer is model dependent. Assuming, for example, a Petschek-type geometry  $\rho_{\text{out}}/\rho_{\text{in}} \sim 2\sigma^{1/2}$  (Lyubarsky 2005), the thickness of the layer is  $\delta \sim l_{\text{rec}} \epsilon / 2\sigma$ .

The downstream magnetic field  $B''$  (in the outflow frame) contributes only a fraction to the total pressure (the rest coming from hot particles). Pressure balance across the reconnection layer, therefore, constrains  $B'' \lesssim B$  (for thermally dominated downstream  $B'' \ll B$ ). In the downstream frame, the preacceleration energy  $E''_{\text{preacc}}$  is given by setting  $\delta = R_g = E''_{\text{preacc}}/eB''$  which yields  $E''_{\text{preacc}} \sim eB'' \delta \lesssim eB \delta \sim eB l_{\text{rec}} \epsilon / 2\sigma$ . For typical GRB parameters and  $\sigma = 100\sigma_2$ ,  $E''_{\text{preacc}} \lesssim 10^{14} \epsilon_{-1}^2 L_{52}^{1/2} \Gamma_{2.5}^{-2} \sigma_2^{-1}$  eV. This is to be compared with the thermal energy in the downstream:  $E''_{\text{thermal}} \sim \sigma^{1/2} m_p c^2 \sim 10^{10} \sigma_2^{1/2}$  eV. Substantial preacceleration above the thermal energy may therefore be required for the mechanism to operate. Tearing instabilities in the current layer are, how-

ever, expected to lead to fluctuations in the thickness of the layer  $\delta$  and to regions where the preacceleration requirements are substantially reduced leading to the bulk of the particle injection.

#### 4 DISCUSSION

Magnetic reconnection results in directly *observed* energetically substantial, non-thermal, high-energy particles during solar flares (Lin & Hudson 1971; Lin et al. 2003) or in Earth's magnetotail (Terasawa & Nishida 1976; Baker & Stone 1976; Øieroset et al. 2002). The puzzling particle acceleration measured by Voyager 1 and Voyager 2 *well* beyond the termination shock of the solar wind (Stone et al. 2005; 2008) may take place at reconnection regions in the shocked solar wind (Lazarian & Opher 2009; Drake et al. 2010). Beyond our solar system, magnetic reconnection may operate in a variety of relativistic environments accelerating particles. Magnetic reconnection in the pulsar winds (Coroniti 1990; Lyubarsky & Kirk 2001), the termination shock of pulsar winds (Lyubarsky 2003) or GRB flows (Thompson 2006) may result in particle acceleration and emission from these sources. If MHD jets contain field reversals on sufficiently small scale (of the order of the light cylinder), reconnection can efficiently power the GRB (Sprit et al. 2001; Drenkhahn & Spruit 2002; Giannios 2008) and AGN jet emission (Sikora et al. 2005; Giannios, Uzdensky & Begelman 2009, 2010; Nalewajko et al. 2010).

Here, I present a model for UHECR acceleration in magnetic reconnection regions in strongly magnetized (AGN or GRB) jets. I argue that the converging magnetized plasma offers an ideal trap for particles to be accelerated to the highest observed energies. The mechanism discussed here assumes that reconnection is fast  $\beta_{\text{rec}} \sim (0.1 - 0.2)\beta_A$  but does not depend on, poorly known, reconnection physics. It is an efficient mechanism that accelerates particles on a timescale of order of their gyration period. Protons can reach  $\sim 10^{20}$  eV in GRB and luminous AGN jets.

#### ACKNOWLEDGMENTS

I thank L. Sironi, A. Spitkovsky, H. C. Spruit, D. A. Uzdensky for important comments and suggestions. I acknowledge support from the Lyman Spitzer, Jr. Fellowship awarded by the Department of Astrophysical Sciences at Princeton University.

#### REFERENCES

Abbasi R. U. et al., 2008, Physical Review Letters, 100, 101101  
 Abraham J. et al., 2008, Physical Review Letters, 101, 061101  
 Achterberg A., Gallant Y. A., Kirk J. G., Guthmann A. W., 2001, MNRAS, 328, 393  
 Baker D. N., Stone E. C., 1976, Geophysical Research Letters, 3, 55  
 Coroniti F. V., 1990, ApJ, 349, 538  
 de Gouveia dal Pino E. M., Lazarian A., 2005, A&A, 441, 845  
 Dermer C. D., Razzaque S., 2010, ApJ, submitted, arXiv:1004.4249  
 Drake J. F., Swisdak M., Che H., Shay M. A., 2006, Nature, 443, 553  
 Drake J. F., Opher M., Swisdak M., Chamoun J. N. 2010, ApJ, 709, 963  
 Drenkhahn G., 2002, A&A, 387, 714  
 Drenkhahn G., Spruit H. C., 2002, A&A, 391, 1141

Farrar G. R., Gruzinov A., 2009, ApJ, 693, 329  
 Gallant Y. A., Achterberg A. 1999, MNRAS, 305, L6  
 Ghisellini G., Ghirlanda G., Tavecchio F., Fraternali F., Pareschi G., 2008, MNRAS, 390, L88  
 Giannios D., 2008, A&A, 480, 305  
 Giannios D., Uzdensky D. A., Begelman M. C., 2009, MNRAS, 395, L29  
 Giannios D., Uzdensky D. A., Begelman M. C., 2010, MNRAS, 402, 1649  
 Greisen K., 1966, Physical Review Letters, 16, 748  
 Guetta D., Piran T., Waxman E., 2005, ApJ, 619, 412  
 Halzen F., Hooper D., 2002, Reports on Progress in Physics, 65, 1025  
 Hillas A. M., 1984, ARA&A, 22, 425  
 Honda M., 2009, ApJ, 706, 1517  
 Inoue, S. 2008, Journal of Physics Conference Series, 120, 062001  
 Kirk J. G., 2004, Physical Review Letters, 92, 181101  
 Kirk J. G., Reville B., 2010, ApJ, 710, L16  
 Lazarian A., Vishniac E. T., 1999, ApJ, 517, 700  
 Lazarian A., Opher M., 2009, ApJ, 703, 8  
 Lin R. P., Hudson H. S., 1971, Solar Pysics, 17, 412  
 Lin R. P. et al. 2003, ApJ, 595, L69  
 Lithwick Y., Sari R., 2001, ApJ, 555, 540  
 Loureiro N. F., Schekochihin A. A., Cowley S. C., 2007, Physics of Plasmas, 14, 100703  
 Loureiro N. F., Uzdensky D. A., Schekochihin A. A., Cowley S. C., Yousef T. A., 2009, MNRAS, 399, L146  
 Lyubarsky Y. E., 2003, MNRAS, 345, 153  
 Lyubarsky Y. E., 2005, MNRAS, 358, 113  
 Lyubarsky Y., Kirk J. G., 2001, ApJ, 547, 437  
 Matthaeus, W. H., & Lamkin, S. L. 1986, Physics of Fluids, 29, 2513  
 Milgrom M., Usov V. 1995, ApJ, 449, L37  
 Murase K., Ioka K., Nagataki S., Nakamura T., 2006, ApJ, 651, L5  
 Murase K., Ioka K., Nagataki S., Nakamura T., 2008, Phys. Rev. D, 78, 023005  
 Nalewajko K., Giannios D., Begelman M. C., Uzdensky D. A., Sikora M. 2010, MNRAS, submitted, arXiv:1007.3994  
 Øieroset M., Lin R. P., Phan T. D., Larson D. E., Bale S. D., 2002, Phys. Rev. Letters, 89, 195001  
 Parker E. N., 1957, Journal of Geophysical Research, 62, 509  
 Pe'er A., Murase K., Mészáros P., 2009, Phys. Rev. D, 80, 123018  
 Petschek H. E., 1964, The Physics of Solar Flares, 425  
 Rieger F. M., Duffy P., 2005, ApJ, 632, L21  
 Samtaney R., Loureiro N. F., Uzdensky D. A., Schekochihin A. A., Cowley S. C., 2009, Physical Review Letters, 103, 105004  
 Sikora M., Begelman M. C., Madejski G. M., Lasota J.-P., 2005, ApJ, 625, 72  
 Sironi L., Spitkovsky A., 2009, ApJ, 698, 1523  
 Speiser T. W., 1965, Journal of Geophysical Research, 70, 4219  
 Spruit H. C., Daigne F., Drenkhahn G., 2001, A&A, 369, 694  
 Stone E. C., Cummings A. C., McDonald F. B., Heikkilä B. C., Lal N., Webber W. R., 2005, Science, 309, 2017  
 Stone E. C., Cummings A. C., McDonald F. B., Heikkilä B. C., Lal N., Webber W. R., 2008, Nature, 454, 71  
 Sweet P. A., 1958, Electromagnetic Phenomena in Cosmical Physics, 6, 123  
 Terasawa T., Nishida A., 1976, Planetary & Space Science, 24, 855  
 Thompson C., 2006, ApJ, 651, 333

- Vietri M., 1995, *ApJ*, 453, 883  
Waxman E., 1995, *Physical Review Letters*, 75, 386  
Waxman E., Loeb A., 2009, *Journal of Cosmology and Astro-Particle Physics*, 8, 2  
Zatsepin G. T., Kuz'min V. A., 1966, *Soviet Journal of Experimental and Theoretical Physics Letters*, 4, 78  
Zenitani S., Hesse M., Klimas A., 2009, *ApJ*, 696, 1385